ISSN: 0369-8963

Multi-operating-condition adaptability enhancement:

Simulation and Experimental Study on the Roof Beam Structure

of Hydraulic Support

Yang Liu, Guozhu Liu, Jingxi Li, Zhen Yadong and Wei Jiang
Yang Liu1,a\*,School of Mechanical and Electrical Engineering, China University of
Mining and Technology -Beijing, Beijing 100083, China,Email: ly ccbj@163.com

Abstract: The mechanical properties of the roof beam structure of hydraulic supports directly affect the safety of support. This paper takes the roof beam of ZY14790/15/25D hydraulic support as the research object, establishes a finite element model through ANSYS software, analyzes the stress and deformation laws of the roof beam under three working conditions: symmetric bending, diagonal torsion, and bending-torsion combination, and identifies the weak areas with stress concentration and large deformation of the roof beam under different working conditions. Based on the analysis results, an optimization technology centered on "enhancing structural continuity, optimizing the load-bearing efficiency of ribs, and strengthening local load-resistant capacity" is proposed, and four optimization schemes are constructed. A new roof beam model is established based on the above schemes, and finite element simulation and cyclic loading comparison tests are carried out. The results show that the maximum stress of the optimized roof beam under the three working conditions is reduced by 31.44%, 19.28%, and 27.20% respectively, the stress distribution is more uniform, and

ISSN: 0369-8963

the maximum deformation is reduced by 12.91%, 12.26%, and 15.63% respectively.

The test shows that the original roof beam fractures after a total of 16,522 cycles, and

the fracture position is at the joint of the top plate and the internal reinforcing plate; the

optimized roof beam has a weld crack that extends to the base metal after 19,100 cycles.

After standardized repair, it continues to complete the remaining cycles and can stably

bear the full yield load, meeting the requirements of actual working conditions. This

study provides a practical scheme for the structural optimization of the roof beam of

hydraulic supports and has reference value for improving the reliability of coal mining

equipment.

**Keywords:** FEM; Optimization Design; Hydraulic Support; Top Beam

## 1. INTRODUCTION

At present, the mechanization level and mining intensity of coal enterprises are increasing year by year. Mine hydraulic supports, with their strong supporting capacity and flexible adaptability, build a safe and reliable working space for the cutting operation of shearers and the material transfer of scraper conveyors, and are the key guarantee for coal mines to achieve high-yield and efficient mining [1]. However, as coal resource mining continues to extend to deep areas, the geological environment faced by mines is becoming increasingly severe. The support work of the mining face, as a weak link in underground production safety, is frequently affected by extreme working conditions such as high ground stress, strong rock burst, and large roof deformation, which put strict requirements on the structural bearing performance, deformation resistance, and load response characteristics of hydraulic supports [2].

The complex structure of hydraulic supports, complex and changeable underground forces, and diverse failure forms bring great difficulties to the failure analysis of the overall structure. Early research on hydraulic supports mainly focused on the failure forms and causes of key load-bearing components of hydraulic supports. Duan et al. [3] found that the humid underground environment and harmful gases such as CH4 and SO2 caused corrosion pits, bubbles, and cracks on the surface of the column, and even 1 mm thick iron plating fell off; Li et al. [4] analyzed the failure of 27SiMn quenched and tempered steel column jacks, and believed that it was due to improper heat treatment leading to substandard mechanical properties, no tempered sorbite in the microstructure, and the fracture showed fatigue striations and dimples, which belonged

ISSN: 0369-8963

to fatigue failure; Zhang et al. [5] pointed out that column socket cracks were caused by the high carbon and manganese content of ZG30SiMn steel, and the high quenching temperature led to grain coarsening and thermal stress concentration; Wang et al. [6] summarized that the ZY7600/24/50 support had top beam column cap welding failure and shield beam fracture due to insufficient strength design, backward welding technology, and poor steel plate quality; Li [7] summarized that the hydraulic support top beam had side guard plate cracking and column cap crushing due to weld thermal stress concentration. In general, the failure forms of hydraulic supports can be divided into corrosion, fatigue fracture, and plastic deformation. However, early studies only simply summarized the failure forms of structural parts, and systematic research and explanation of the failure causes of major components of the support are still rare, and the complex conditions of underground operations are not considered. Therefore, researchers have begun to pay attention to the bearing process and failure analysis of key load-bearing components of hydraulic supports under different working conditions. Xia et al. [8] conducted a finite element analysis on the jack and column of ZY5200/8/18D, and compared the finite element results with the analytical calculation results. It was found that the stress conditions under various load conditions were basically consistent, verifying the effectiveness of finite element calculation. LIU et al. [9], with reference to the MT312—2000 standard, conducted a finite element analysis on the prototype of ZT6500/19.5/34 hydraulic support and its 1:5 simplified model under the condition of loading in the middle of the top beam. The test results showed that the displacement of the front part of the top beam was the largest, decreasing

ISSN: 0369-8963

towards the rear; The stress of the connecting pin between the top beam and the connecting rod was the largest, 217 MPa, which was lower than the yield strength of 40Cr steel. Chen et al. [10], based on GB 25974.1—2010, conducted a finite element analysis on the entire ZY6400/21/45 hydraulic support under two single load conditions: top beam torsion and top beam eccentricity [11]. The results showed that there was a potential safety hazard at the connection of the jack ear plate on the shield beam under the eccentric load condition. He et al. [12] studied the stress distribution of the top beam and base of ZF6400/19/32 hydraulic support under two composite working conditions, and found that under the composite working condition of top beam bending loading and base horizontal loading, the maximum stress value of the base appeared at the arc transition of the main rib plate, which was 614 MPa, exceeding the yield strength of Q460; Under the composite working condition of top beam torsion loading and base bending loading, there was stress concentration around the top beam hole, and the stress value exceeded the yield strength of Q460. Zhao et al. [13] studied the stress distribution of main components under the composite working condition of top beam torsion loading and base two-end loading. The test results showed that the maximum stress value of the entire support appeared on the top beam, and the high stress areas of the top beam were mainly in the pin holes, column caps, and box structures; The stress of the base showed a symmetrical distribution, and the high stress areas were concentrated at the arc transition of the main rib plate, column sockets, and their box structures; The high stress of the shield beam was reflected in the pin holes connecting the jack, between the cover plate and the main rib plate, and the main welding parts.

ISSN: 0369-8963

As the key load-bearing component of the hydraulic support that directly contacts the roof, the top beam bears huge pressure from the roof, impact loads, and complex bending moments for a long time. The rationality of its structural design is directly related to the overall support effect and safety reliability of the support. As the "skeleton structure" inside the top beam, the rationality of the distribution position and the adaptability of the structural form of the reinforcing ribs are the core factors determining the overall stiffness, stress transfer efficiency, and fatigue resistance of the top beam. In the traditional top beam design, reinforcing ribs mostly adopt equidistant symmetrical distribution or extensive arrangement based on experience. This design is difficult to achieve uniform stress transfer and efficient structural bearing when facing complex and variable roof loads, often leading to serious stress concentration in local areas due to insufficient reinforcement, which in turn leads to damage and failure of the top beam. Therefore, to further improve the support performance of hydraulic supports, it is necessary to carry out finite element strength and deformation analysis of the hydraulic support top beam structure under multiple working conditions, extract corresponding calculation results, optimize the structural dimensions of local weak links, and conduct test verification [14].

In recent years, scholars at home and abroad have carried out a lot of research on the optimization of hydraulic support top beams. Zhong et al. [15] aimed at the stability problem of large-inclination hydraulic supports, and verified through mechanical modeling that when the coal seam inclination is  $31^{\circ}$  and the downward inclination is  $10^{\circ}$ , the minimum anti-overturning support resistance must be  $\geq 283.59$  kN, and the

ISSN: 0369-8963

critical resistance increases approximately linearly with mining height and inclination, providing key theoretical basis for support design. He et al. [16] studied the stress distribution characteristics of ZF6400/19/32 hydraulic support under two combined working conditions: top beam bending and base horizontal loading, and top beam rear torsion and base bending. Through constructing a simplified model and ABAQUS finite element analysis, the dangerous and weak areas of the hydraulic support were determined, and then the original structural design was optimized. The research results showed that the improved scheme met the strength requirements and improved the working safety and reliability of this type of hydraulic support. Wang [17] analyzed the top beam based on the ABAQUS topology optimization module, and optimized the structure of the top beam according to the topology optimization results and the problems in the actual use of the hydraulic support. The stress calculation results of the optimized structure showed that compared with the original structure, the maximum stress value under torsion condition was 442.9 MPa, which was reduced by 65.8 MPa.

Although certain research results have been achieved in the topological structure design of hydraulic supports at home and abroad, there are still obvious limitations and difficulties. Existing studies mostly focus on the optimization design of reinforcing ribs under a single working condition, while the exploration in the fields of bearing analysis, fatigue performance research of top beams under multiple working conditions, and topology optimization of top beam reinforcing ribs is still weak. Specifically, current research often focuses on specific working conditions, which is difficult to adapt to complex multi-working conditions such as dynamic fluctuation of roof load, change of

ISSN: 0369-8963

support height, and asymmetric eccentric load in mines; As a core load-bearing component, the top beam lacks systematic research on stress distribution and fatigue damage accumulation mechanism under alternating loads, making it difficult to accurately predict its fatigue life; The topology optimization of reinforcing ribs is also mostly based on single working condition objectives, without fully considering the differential requirements of different load modes on the layout under multiple working conditions, which is prone to local overload or material waste, and it is difficult to achieve the optimal comprehensive performance. These deficiencies not only restrict theoretical development but also affect the adaptability and service life of products in engineering applications.

To address the above problems, this paper focuses on the optimization design of the top beam structure of mine hydraulic supports, taking the distribution position and structural size of reinforcing ribs as the core optimization objects. Taking ZY14790/15/25D mine hydraulic support as an example, through constructing its simplified model and conducting finite element simulation analysis, the stress field distribution law of its top beam under various complex working conditions is analyzed, the weak links of the top beam structure are found, and the collaborative optimization scheme of rib layout and structural size is explored. In addition, based on the simulation results, the internal relationship between reinforcing ribs and load transfer is revealed, and iterative design, such as topology and thickening, is further carried out on some rib plates of the top beam. The reliability of the iterative design is verified by test, aiming to achieve multi-objective optimization of load adaptation and stress balance. This

ISSN: 0369-8963

research has important reference value for enhancing the operational stability and support safety of this type of hydraulic support, and also provides a solid theoretical support and technical reference for the engineering application of high-reliability top beams.

## 2. MODEL CONSTRUCTION AND SIMULATION

In underground projects such as coal mining, hydraulic supports are important equipment to ensure the safety and stability of the working face. This paper takes the ZY14790/12/25D two-column shield hydraulic support used in coal mines as the research object. This type of hydraulic support is a full-mechanized mining hydraulic support for medium-thick coal seams with a single mining height, with a working resistance of 14790 KN, a center distance of 2.05 m, and a support strength of 1.1-1.2 MPa. Figure 1 shows the schematic diagram of the main structure of the mine hydraulic support. It can be seen that the structural parts of the hydraulic support mainly include the top beam, base, shield beam, front and rear connecting rods, and hydraulic columns. Any mechanical structure must bear large loads during operation, so it must have sufficient comprehensive mechanical properties. As a key component of the hydraulic support, the top beam plays a crucial role. Its main function is to bear the huge pressure from the roof or the impact of falling gangue, ensuring the stability and safety of the working face. Therefore, the structural design of the top beam is not only related to the bearing capacity of the hydraulic support but also directly related to its overall stability.

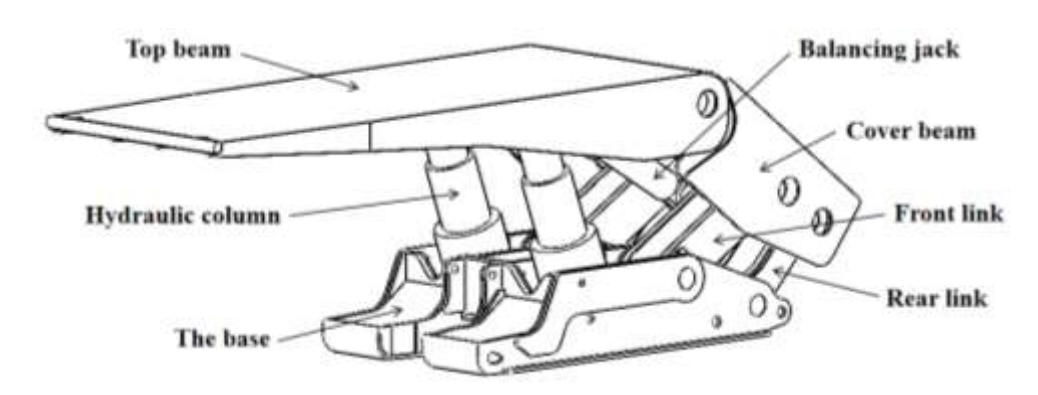


Figure 1 Schematic diagram of the main structure of mine hydraulic support

## 2.1 Construction of Simplified Model of Hydraulic Support

In the construction of the hydraulic support structure model, to reduce the model calculation time and ensure the convergence of the calculation process, it is necessary to simplify some detailed structures [4]. The following principles are adopted for simplifying the hydraulic support model [18,19]. Firstly, in terms of similarity, the integrity of the main quantitative structure must be ensured during simplification, and the simplified model should not affect the strength of the top beam. Secondly, the simplified model should be able to carry out finite element analysis smoothly without affecting the quality of mesh division and the verifiability of results. Finally, ensure the recoverability of the entity. When entity reduction display is needed, the original entity can be found through the assembly path.

Therefore, this paper uses Solidworks software to establish a 3D model according to the actual size of the hydraulic support structure. During modeling, the above principles are strictly followed, and both analysis efficiency and accuracy are considered. Auxiliary features such as chamfers and small holes that do not affect the structure and strength are removed, only the key components of the load-bearing structural parts are retained, non-load-bearing components such as oil pipes and guard

plates are omitted, and the balance jack is simplified as a solid column, whose length is determined by the working height of the hydraulic support. The main component sizes of all parts of the hydraulic support remain unchanged, and the column sockets with potential stress are not simplified. Finally, the simplified model of ZY14790/15/25D hydraulic support as shown in Figure 2 is obtained.

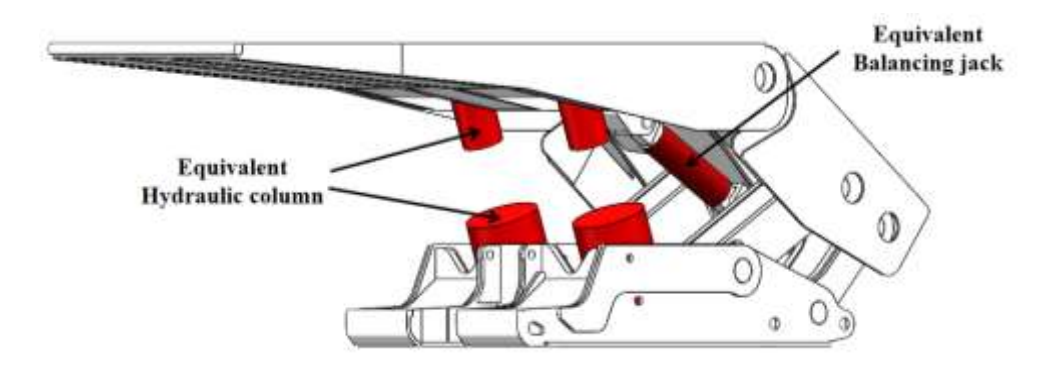


Figure 2 Simplified model of ZY14790/15/25/D

# 2.2 Finite Element Simulation Design

The simplified model of the hydraulic support constructed in Section 2.1 is imported into ANSYS software, and material parameters are assigned to the model in the software. Although the steel used in hydraulic support design is not uniform, the differences in density, elastic modulus, and Poisson's ratio of various steels are small. To better simulate the real situation of the hydraulic support during use, the simulation material is set to Q690, and the relevant parameters of this material are shown in Table 1. This material is applied to all components of the hydraulic support.

Table 1 Q690 material parameters

Elastic	Poisson's	Density	Tensile Strength	Yield Strength
Modulus (GPa)	Ratio	(Kg/m³)	(MPa)	(MPa)
210	0.3	7850	900	690

For mesh division of the finite element model, tetrahedral mesh type is selected for this model. Through mesh convergence test, the mesh element size is set to 50 mm, and at the same time, to improve the convergence or accuracy of the calculation results, the boundary mesh is encrypted. The finite element mesh division of the hydraulic support model is shown in Figure 3.

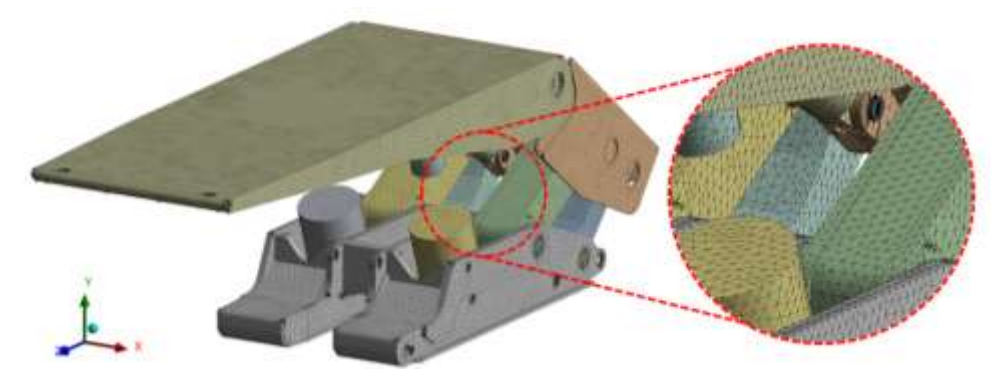


Figure 3 Schematic diagram of mesh division of hydraulic support model

In applying constraints, the method of placing heel blocks at different positions of the hydraulic support top beam is used to simulate different underground bearing working conditions. According to the Chinese standard GB-25974.1-2010 [11], the placement of heel blocks on the top beam corresponding to the three working conditions of symmetric bending, bending-torsion combination, and diagonal torsion is shown in Figure 4. Since this paper focuses on the top beam structure and considers controlling other influencing factors, the placement of heel blocks on the base under the three working conditions is unified as two-end loading placement.

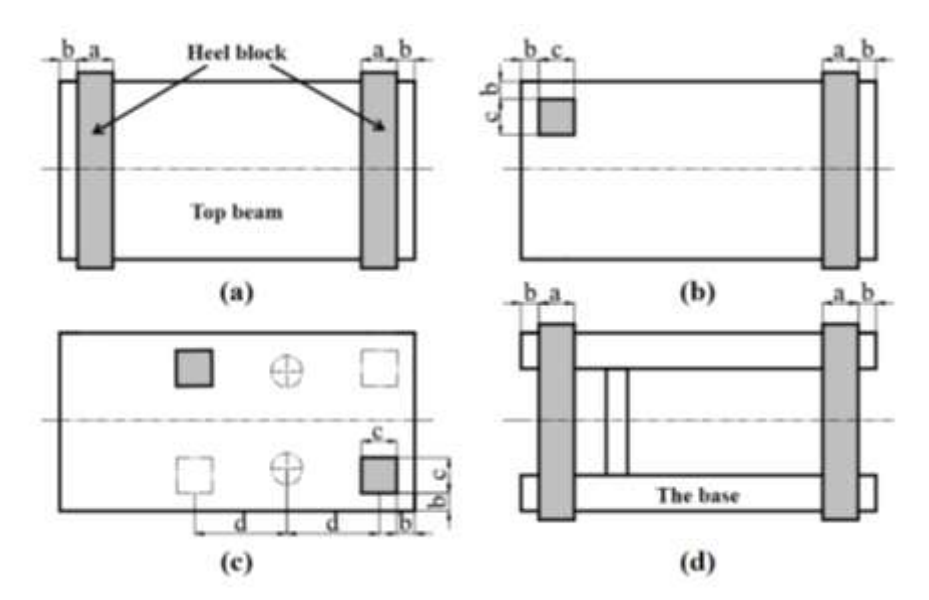


Figure 4 Placement of heel blocks of hydraulic support under different working conditions (a) Position of heel block on top beam during symmetric bending; (b) Position of heel block on top beam during bending-torsion combination; (c) Position of heel block on top beam during diagonal torsion; (d) Position of heel block on base under different working conditions; (a=150 mm; b=50 mm; c=300 mm; d=2630 mm; thickness, h=50 mm)

In addition, according to the Chinese standard GB-25974.1-2010, the load should be applied to the heel block, and the force generated by the heel block on the hydraulic support is regarded as the load condition in the finite element analysis. However, it is difficult to determine the surface load of the heel block based on the rated working resistance of the column, and statically indeterminate problems may occur in the finite element analysis. Therefore, in establishing the simplified model, the hydraulic column is simplified into two parts near the top column socket and the bottom contact part. Since the structure of the heel block is used as a boundary constraint condition, and the load application mode of the hydraulic support strength test is the internal load application mode, the external load is applied to the circular end faces of the two columns [13]. When the top beam bears the load and the two ends of the base bear the load, the relevant parameters of the finite element simulation of the hydraulic support are calculated according to the following formulas.

According to the model of the hydraulic support, the stroke (L) of the hydraulic support is 1000 mm, and the test height (H) of the hydraulic support is:

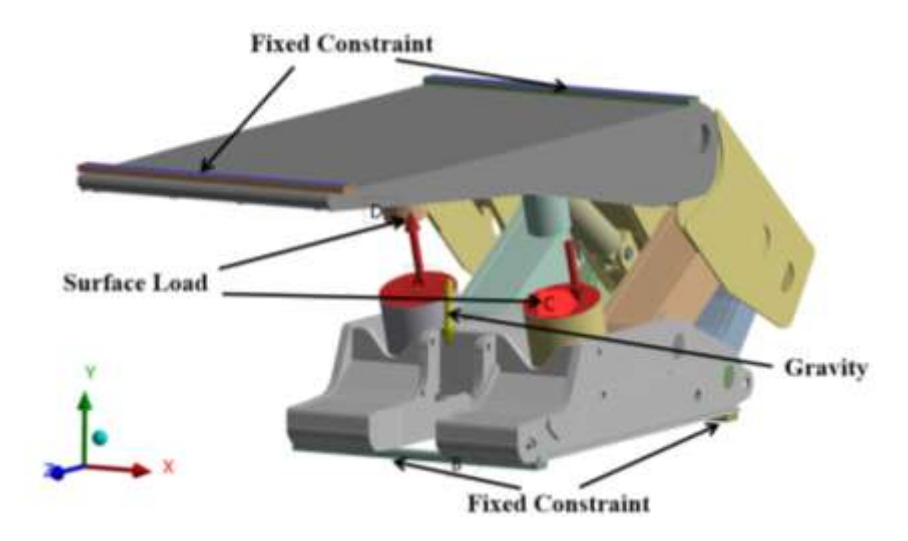
$$H=H_{\text{max}}-L/3=2500-1000/3\text{mm}=2167\text{mm}$$
 (1)

According to the Chinese standard GB-25974.1-2010, the rated working resistance  $(F_r)$  of a single column of this type of hydraulic support is 7395 kN, and the actual load  $(F_a)$  is 1.2 times the rated load, which is 8874 KN. The diameters of the live column and the outer cylinder are 295 mm and 530 mm respectively, so the surface loads of the live column and the outer cylinder are:

$$P_1 = F_a/S_1 = 8.874 \times 10^6/(\pi \times 295^2/4) \text{ mm}^2 = 129.84 \text{MPa}$$
 (2)

$$P_2 = F_a / S_2 = 8.874 \times 10^6 / (\pi \times 530^2 / 4) \text{ mm}^2 = 40.23 \text{MPa}$$
 (3)

The above constraint conditions are applied to the finite element model of the hydraulic support. Taking the two-end loading of the top beam as an example, the loading situation is shown in Figure 5. After completing the setting of the boundary conditions of the finite element model, the analysis and calculation module is called to analyze the model, and finally, the post-processing module is called to process the results.



ISSN: 0369-8963

Figure 5 Schematic diagram of boundary conditions and loads of hydraulic support model

## 2.3 Analysis of Top Beam Strength and Deformation Under Multiple Working

#### **Conditions**

Static analysis is an important index to evaluate the comprehensive performance of mechanical structures. For key components such as the rear top beam of hydraulic supports, the analysis results can provide an important basis for structural improvement. The stress nephograms and deformation nephograms of the ZY14790/15/25D hydraulic support model under the working conditions of top beam symmetric bending, top beam bending-torsion combination, and top beam diagonal torsion are analyzed and studied respectively.

## (1) Symmetric bending working condition

As shown in Figure 6(a), under the two-end loading condition, the deformation and stress distribution of the hydraulic support top beam show clear mechanical laws. The deformation distribution is characterized by being large in the middle area and gradually decreasing towards both ends. The maximum deformation occurs in the middle part of the top beam, with a value of 17.44 mm. This situation occurs because the top beam can be regarded as a simply supported beam model under two-end loading. When symmetrically loaded, the bending moment at the mid-span position is the largest, and the bending moment causes the maximum deformation displacement at the mid-span position, and the deformation gradually decreases from the mid-span position to the two-end constraint positions.

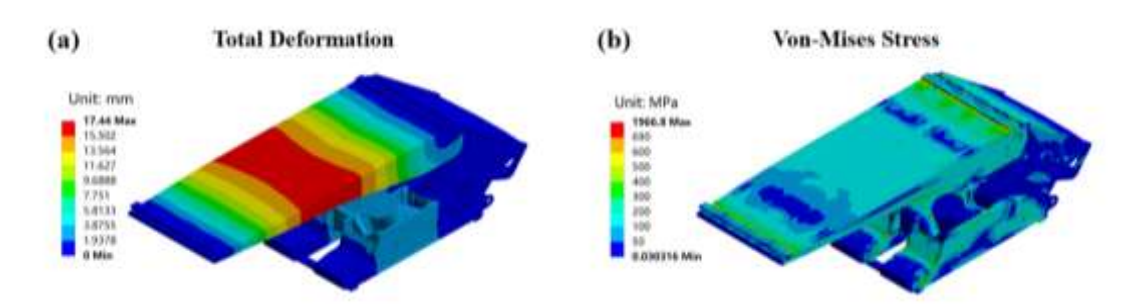


Figure 6 Deformation and stress distribution of hydraulic support top beam during symmetric bending (a) Total deformation nephogram of hydraulic support top beam; (b) Stress nephogram of hydraulic support top beam

In terms of stress distribution, since the top beam needs to be connected with the column, shield beam, and other components to transfer force, the force transfer path changes at the connection part, and the geometric shape of the hydraulic support structure changes suddenly, resulting in stress concentration. At the same time, the edge of the top beam is affected by the change of stress state of the tension and compression fiber layers during bending deformation, and the geometric discontinuities such as chamfers and welds existing in the actual hydraulic support also cause local stress concentration, making the two-end connection parts and local edges high stress areas, with the maximum equivalent stress of 1966.8 MPa; The middle area of the top beam mainly bears bending normal stress, and the stress distribution is relatively uniform. Due to the large structural size, the stress is dispersed, and the stress value is lower than that of local areas such as the two-end connections.

#### (2) Diagonal torsion working condition

Under the diagonal torsion loading condition, the total deformation of the top beam shows a gradient distribution along the torsion direction. As shown in Figure 7(a), due to the diagonal torsion load of the top beam, the torque causes the top beam to produce torsional deformation around the diagonal. The fixed heel block limits the displacement

of the constrained area, and the deformation gradually increases from the constrained position to the diagonal area driven by torsion. The maximum deformation of 13.517 mm is concentrated in the diagonal part far from the constraint.

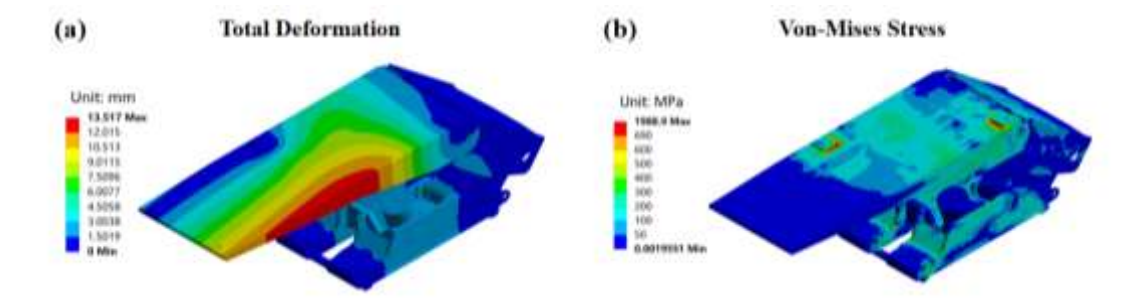


Figure 7 Deformation and stress distribution of hydraulic support top beam during diagonal torsion(a) Total deformation nephogram of hydraulic support top beam; (b) Stress nephogram of hydraulic support top beam

It can be seen from the stress nephogram of the hydraulic support top beam in Figure 7(b) that the maximum equivalent stress reaches 1988.9 MPa, and the equivalent stress is concentrated in the connection structure of the top beam. Torsion causes a complex stress field coupling shear stress and bending stress inside the top beam, and the connection part needs to transfer the torsional moment, so the force flow converges here. At the sudden change of the geometric structure, the stress lines cannot transition smoothly, resulting in a sharp increase in local stress and stress concentration.

#### (3) Bending-torsion combination working condition

Under the bending-torsion condition of the hydraulic support top beam with twoend loading, the total deformation nephogram shows an uneven distribution characteristic. The maximum deformation reaches 25.48 mm, which appears on the side of the top beam without a heel block in the front. From the perspective of mechanical principles, the top beam is subjected to combined bending and torsion loads. Bending produces bending deformation along the loading direction, and torsion causes torsional

deformation around the beam axis. The superposition of the two makes the deformation distribution complex. Since the heel block acts as a fixed support, it limits local displacement and makes the deformation at the constraint small, while the deformation in the area far from the constraint gradually increases under the combined action of bending and torsion loads.

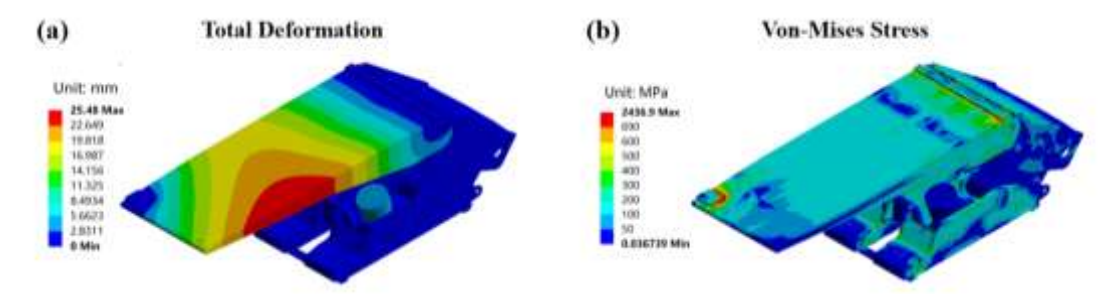


Figure 8 Deformation and stress distribution of hydraulic support top beam during bending-torsion combination(a) Total deformation nephogram of hydraulic support top beam; (b) Stress nephogram of hydraulic support top beam

The equivalent stress nephogram of the top beam in Figure 8(b) shows that the stress distribution is also uneven. The maximum equivalent stress of the structure is 2436.9 MPa, which is concentrated in the connection part between the top beam and other components and some edges. This is because under the bending-torsion load, the top beam not only bears bending normal stress and shear stress but also generates torsional shear stress due to torsion. The superposition of various stresses causes the stress in areas such as the connection between the top beam and other components to increase sharply, directly affecting the safety of the entire support.

# 3. OPTIMIZATION AND VERIFICATION OF TOP BEAM STRUCTURE

According to the simulation results in Section 2.3, it can be seen that under the three different working conditions, the top beam of the hydraulic support is the weak

part of the entire structure. If the external load, working conditions, or equipment processing problems change, the hydraulic support is prone to structural failure, which seriously affects the safety of underground support. Therefore, in the structural optimization of the hydraulic support model, the optimization design of the top beam structure should be taken as the key research part.

## 3.1 Improvement Ideas Of Top Beam Structure

In the optimization design stage of ZY14790/12/25D hydraulic support, combined with the simulation results of the original top beam model and considering the characteristics of the hydraulic support structure, the top beam is focused on structural strengthening. Therefore, the following improvement designs are proposed for the top beam model of this type of hydraulic support from multiple angles, and finally, the iteratively designed new top beam model of this type is obtained:

Design 1: The original top beam model was composed of steel plate 1 (gray) with a thickness of 25 mm and steel plate 2 (red) with a thickness of 30 mm. The new top beam model combines the two parts and uses an integral steel plate 3 (green) with a thickness of 40 mm. The above improvement is made because there are welds or connection gaps at the joint of the combined steel plates of the original top beam model, which are prone to stress concentration due to discontinuous force flow transfer during bearing, and long-term loading may lead to weld cracking. The integral steel plate can eliminate the splicing structure, make the stress transfer uniformly along the plate, and reduce the risk of local fracture; At the same time, the integral thick steel plate has better section continuity, which can disperse the load more uniformly under bending, torsion,

ISSN: 0369-8963

and other working conditions, and has stronger deformation resistance, especially in the area with the maximum bending deformation in the middle of the top beam, which can effectively control the deformation. It can also simplify the manufacturing process, reduce structural hidden dangers caused by fluctuations in welding quality, and improve the manufacturing consistency of the top beam.

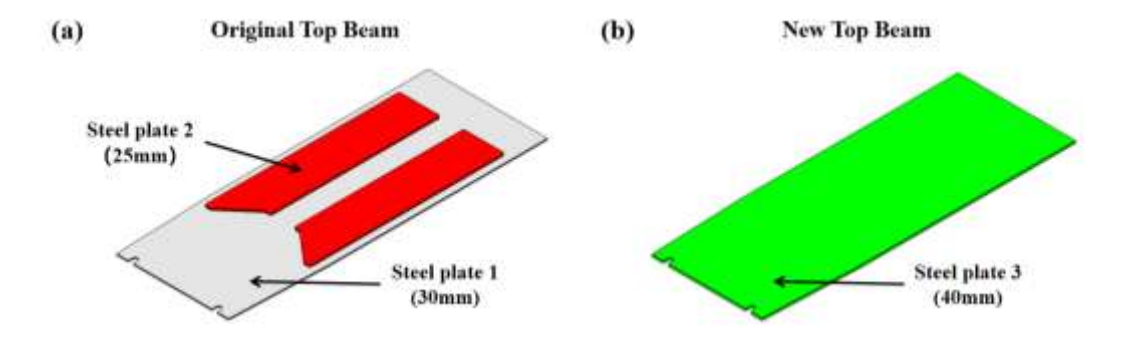


Figure 9 Comparison of old and new top beam models under the first improvement (a) Original top beam design; (b) New top beam design

Design 2: The new top beam model adjusts the arrangement position of the lateral reinforcing plates on both sides, increases the number of arrangements, and increases the thickness of the longitudinal reinforcing plates from 25 mm to 40 mm, exceeding the height of the second layer of the cover plate. This improvement is because the lateral reinforcing plates, as the lateral support of the top beam, can better resist the torque under diagonal torsion conditions after increasing the number and optimizing the position, reducing torsional deformation; In addition, the longitudinal reinforcing plates are the core skeleton of the top beam to bear bending loads. After thickening to 40 mm, the section moment of inertia increases, and the bending strength is significantly improved. The height exceeding the cover plate can further expand the force transfer range, avoid cracking at the joint between the cover plate and the reinforcing plates due to stress concentration, and under the bending-torsion combination condition, the

collaborative effect of lateral and longitudinal reinforcing plates can disperse the composite stress, reducing the overload risk of the connection part.

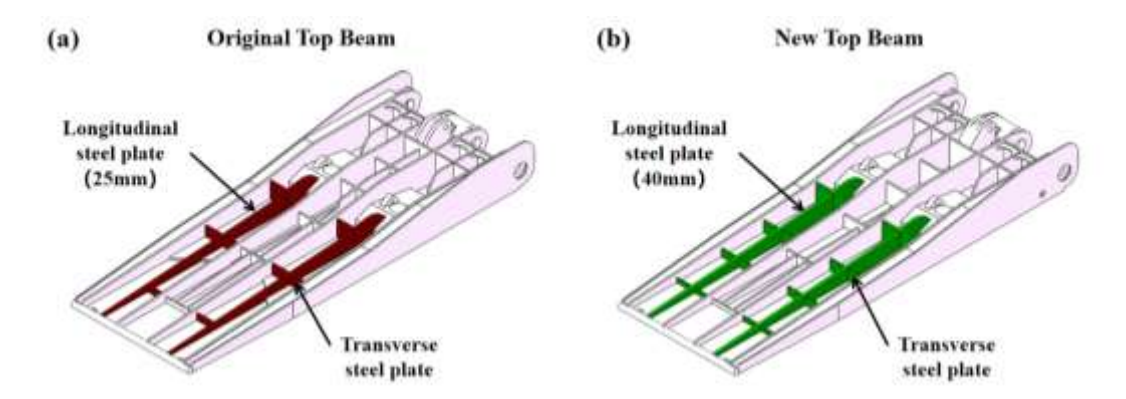


Figure 10 Comparison of old and new top beam models under the second improvement (a) Original top beam design; (b) New top beam design

Design 3: The new top beam model adjusts the middle lateral reinforcing plates, and changes the height of the middle longitudinal reinforcing plates according to the stress distribution. The new top beam optimizes the arrangement of the middle lateral reinforcing plates and adjusts the height of the middle longitudinal reinforcing plates. The reason for Design 3 is that the middle area is the maximum deformation area of the top beam under symmetric bending conditions. Adjusting the middle lateral reinforcing plates can enhance the local support in this area, avoiding plastic deformation caused by excessive bending; The adjustment of the height of the longitudinal reinforcing plates can make the stress distribute more uniformly along the height direction of the reinforcing plates, avoiding stress concentration at the connection edge between the reinforcing plates and the cover plate, guiding the force flow to transfer smoothly from the top plate to the column, reducing local high stress, and this local adjustment can avoid excessive increase in the weight of the top beam while improving the strength of key areas, achieving a balance between lightweight and high strength.

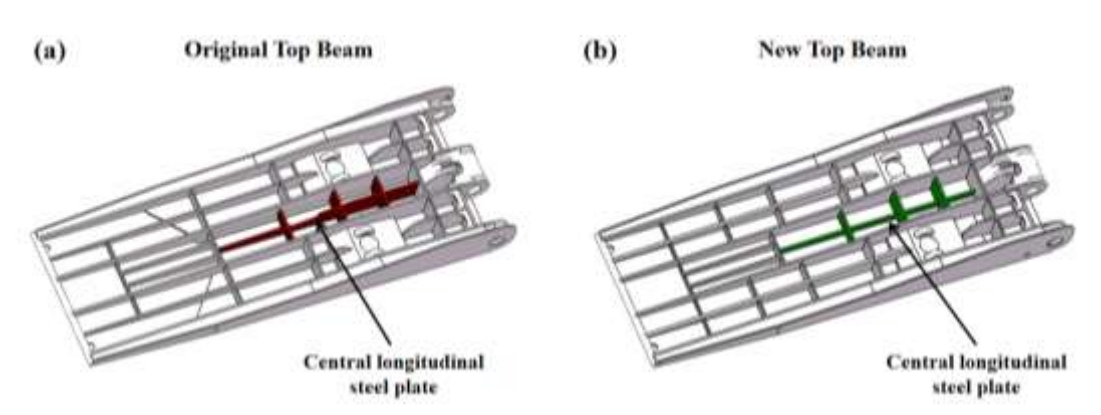


Figure 11 Comparison of old and new top beam models under the third improvement (a) Original top beam design; (b) New top beam design

Design 4: The new top beam model increases the thickness of the inner cover plate from 12 mm to 25 mm and adjusts from two plates to four plates. This improvement is because the inner cover plate bears the pressure and impact load of the top plate. After thickening to 25 mm, the compression and impact resistance of the inner cover plate is enhanced, which can reduce the depression caused by excessive local pressure; Increasing the number of inner cover plates can expand the load contact area, reduce the pressure per unit area, especially under eccentric load or local impact conditions, which can avoid damage to a single cover plate due to excessive force. At the same time, the thickened inner cover plate is more firmly connected with the reinforcing plates, which can improve the shear resistance of the connection part and reduce the risk of weld failure.

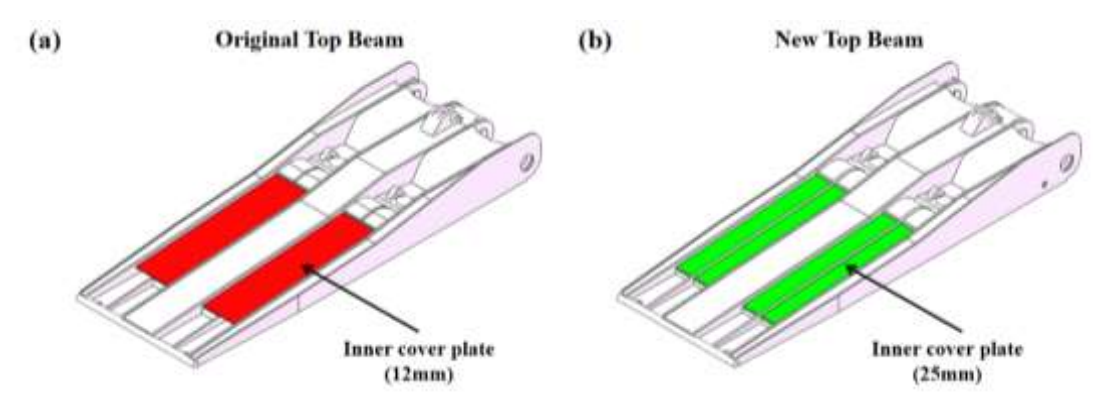


Figure 12 Comparison of old and new top beam models under the fourth improvement (a) Original top beam design; (b) New top beam design

ISSN: 0369-8963

Compared with the original top beam model, the optimization goal of the new top beam model is to minimize the stress of the top beam structure during service, improve the uniformity of stress distribution, reduce stress concentration, improve the safety factor of the rear top beam structure, and lay a good foundation for the safe service of the entire hydraulic support. After obtaining the specific optimization scheme, Solidworks software is used again to model the new top beam model. Except for the size of the optimized parts that need to be changed, the modeling process of other parts is the same as that of the original model. The stress and deformation results of the optimized new top beam model under different working conditions are shown in Section 3.2.

# 3.2 Finite Element Optimization Results

Through targeted optimization of the top beam structure, the mechanical properties of the new top beam model under the three working conditions of symmetric bending, diagonal torsion, and bending-torsion combination are significantly improved. The following combines the simulation nephograms and the deformation and stress data of the two top beam top plate paths, as shown in Figure 13, to compare and analyze the stress magnitude and distribution of the top beam before and after optimization.

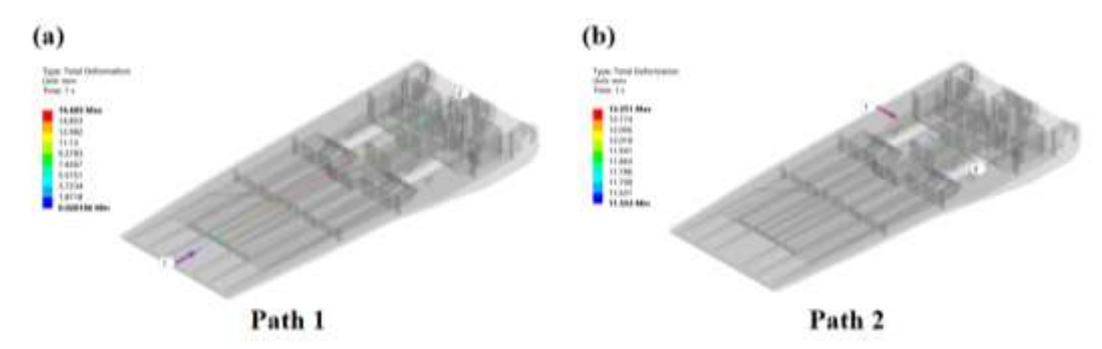


Figure 13 Two key paths of the top beam studied (taking the total deformation of the original top beam under symmetric bending loading as an example)

ISSN: 0369-8963

(a) Path 1: Longitudinal central axis of the top beam; (b) Path 2: Horizontal line passing through the column socket center on the top beam

# 3.2.1 Symmetric Bending Working Condition

The simulation nephogram results in Figure 14 show that the mechanical properties of the new top beam under symmetric bending conditions are significantly improved compared with the original top beam. The original top beam adopts a spliced structure of 25 mm and 30 mm steel plates, and the force flow transfer is interrupted at the weld, resulting in a maximum equivalent stress of up to 1966.8 MPa, and the high stress area is distributed along the splice seam; The new top beam eliminates splicing defects through a 40 mm integral steel plate, and the maximum equivalent stress is reduced to 1348.4 MPa, with a decrease of 31.4 %. At the same time, due to the continuity of the integral steel plate, the force flow diffuses uniformly from the column socket to the main body of the top beam, avoiding the stress fragmentation caused by weld blocking in the original structure. Therefore, the high stress area in the stress nephogram of the new top beam is more uniformly distributed and smaller in range than that of the original top beam. In addition, in terms of deformation, the maximum deformation of the total deformation nephogram of the new top beam is reduced by 26.9 % compared with the original top beam, and the deformation gradient is gentler, reflecting the improvement of the bending stiffness of the overall structure.

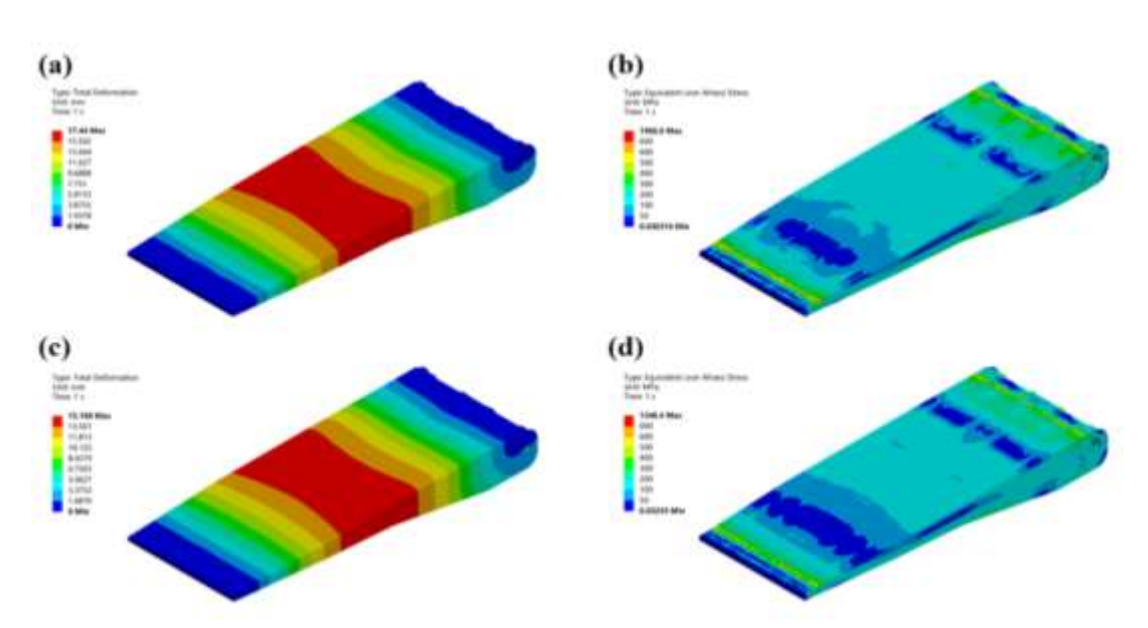


Figure 14 Total deformation and equivalent stress nephograms of old and new top beams under symmetric bendin(a) Total deformation nephogram of original top beam; (b) Stress nephogram of original top beam(c) Total deformation nephogram of new top beam; (d) Stress nephogram of new top beam

It can be seen from Figure 15(a) that the deformation of the old and new top beams on the longitudinal central axis of the top beam (Path 1) both show typical simply supported beam characteristics. From the simulation data, the mid-span displacement peak of the original top beam is prominent, with a maximum deformation of 16.69 mm, while the curve of the new top beam tends to be gentle, with a maximum deformation of 14.64 mm, and the peak value is reduced by 12.26 %. This is because when the top beam is subjected to symmetric bending loading, the mid-span position of the top beam bears the maximum bending moment. The integral steel plate design (Design 1) of the new top beam improves the bending stiffness of the overall section, making the bending load transfer uniformly along the longitudinal central axis, and the deformation is effectively controlled. The stress curve in Figure 15(b) shows that the original design has a steep stress peak near the column socket, while the new design has a more uniform stress distribution due to the thickened longitudinal reinforcing plates and the

ISSN: 0369-8963

application of integral steel plates (Design 2). Compared with the original top beam, the number of stress peaks is reduced, and the maximum peak value is reduced by 16.75 %.

On the horizontal line passing through the column socket center (Path 2), the total deformation trends of the old and new top beams are the same, but the peak value of the total deformation curve of the new top beam is lower than that of the original top beam, and the deformation gradient in the edge area is reduced. In addition, on Path 2, the stress distribution of the original top beam is uneven, and a stress peak of 152.99 MPa appears near the center of the horizontal line at the column socket of the original top beam, while the overall stress distribution of the new top beam is gentler, and the stress value at the center of the horizontal line is 103.93 MPa, without stress concentration. This is because in Design 3, the new top beam adjusts the height of the longitudinal reinforcing plates (Design 3), which can make the stress distribute more uniformly along the height direction of the reinforcing plates, expand the transfer range, and avoid stress concentration at the connection edge between the reinforcing plates and the cover plate, thus reducing the stress peak.

Comparing the optimization effects of the two paths, the reduction in deformation of Path 1 confirms the strengthening effect of the integral steel plate of the new top beam on bending stiffness, and the reduction in stress of Path 2 reflects the optimization of force flow transfer by structural continuity. It further shows that the improved new top beam conforms to the mechanical logic of enhancing mid-span stiffness to control deformation of simply supported beams, solves the problem of stress concentration by

eliminating structural weak points, and makes the bearing performance of the new top beam under symmetric bending conditions more in line with the actual working requirements.

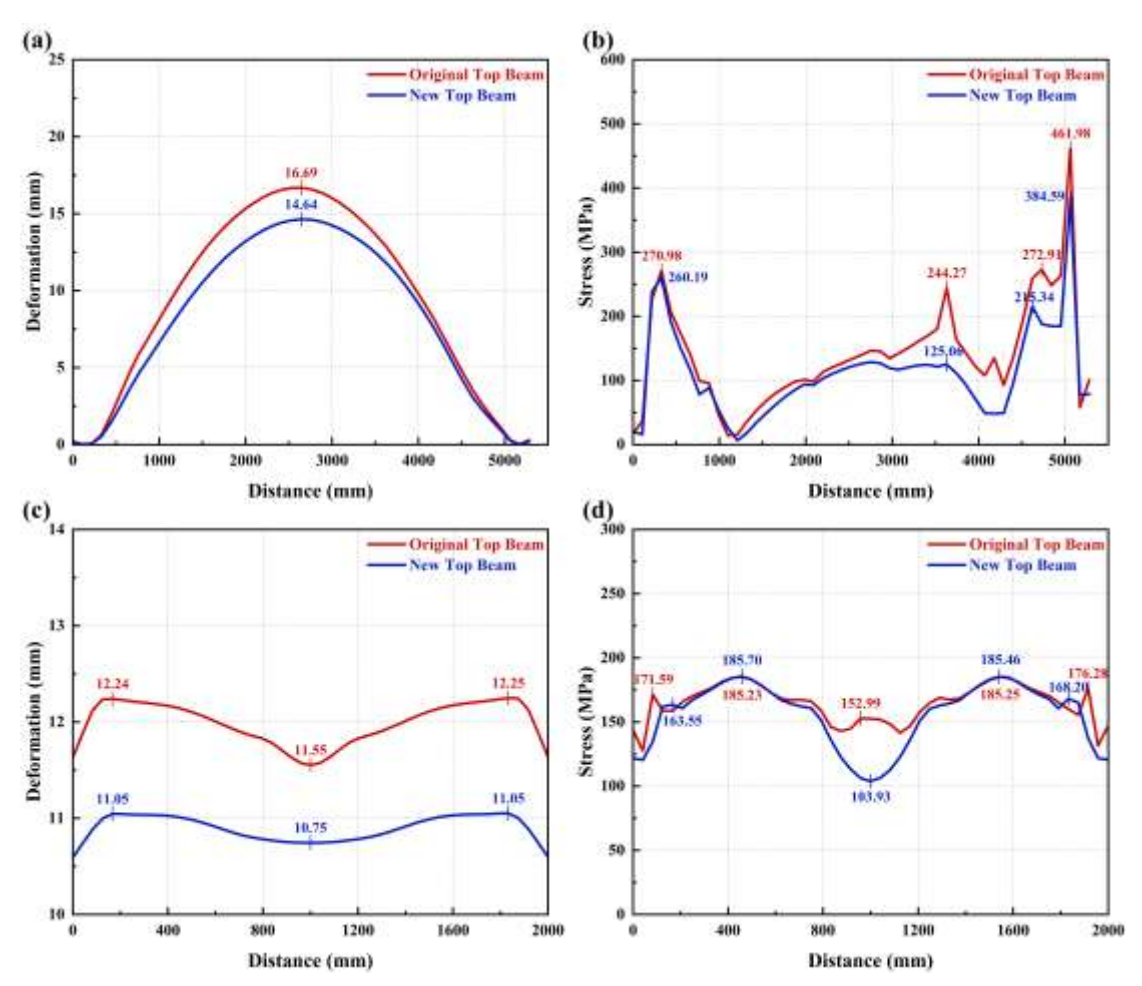


Figure 15 Total deformation and equivalent stress curves of old and new top beam top plates on two paths under symmetric bending loading

(a) Total deformation nephogram of old and new top beams on Path 1; (b) Equivalent stress nephogram of old and new top beams on Path 1; (c) Total deformation nephogram of old and new top beams on Path 2; (d) Equivalent stress nephogram of old and new top beams on Path 2

## 3.2.2 Diagonal Torsion Working Condition

Under diagonal torsion conditions, the new top beam significantly improves its mechanical response through structural optimization. In terms of deformation, due to the torsional deformation of the top beam around the diagonal under torque, the original top beam has insufficient number of lateral reinforcing plates and scattered arrangement,

ISSN: 0369-8963

which cannot effectively resist torsional deformation, resulting in a gradient increase in deformation along the torsion direction. The maximum deformation of the total deformation nephogram of the new top beam is reduced by 12.23 % compared with the original top beam. This is because after the new top beam forms a torsion-resistant grid through lateral reinforcing plates, it effectively blocks the transfer path of torsional deformation, significantly improving the diagonal torsion performance. In terms of stress, the original top beam has a maximum equivalent stress of 1988.9 MPa due to insufficient number of lateral reinforcing plates and a longitudinal reinforcing plate thickness of only 25 mm, and the high stress area is distributed in a band along the diagonal; After increasing the number of lateral reinforcing plates and thickening the longitudinal reinforcing plates to 40 mm, the maximum equivalent stress of the new top beam is reduced to 1605.5 MPa, a decrease of 19.3 %, and the high stress area shrinks to the periphery of the connecting pin hole, with an area smaller than that of the original top beam.

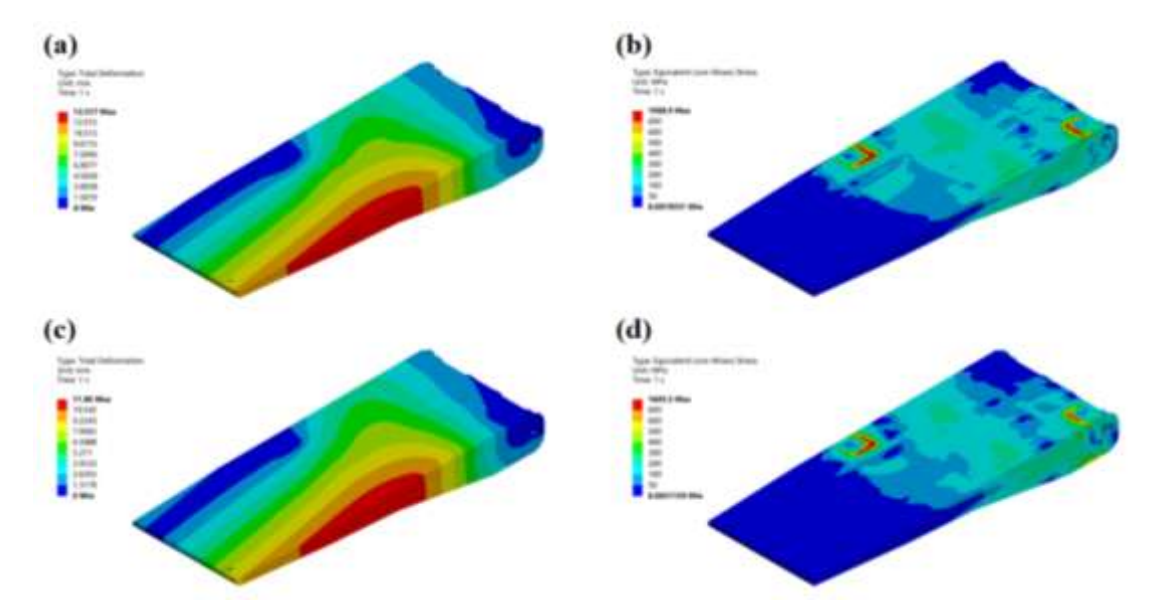


Figure 16 Total deformation and equivalent stress nephograms of old and new top beams under diagonal torsion

ISSN: 0369-8963

(a) Total deformation nephogram of original top beam; (b) Stress nephogram of original top beam (c) Total deformation nephogram of new top beam; (d) Stress nephogram of new top beam

The path curves in Figure 17 further reveal the optimization mechanism. On Path 1, the deformation of the original top beam increases from the constrained end to the torsion end, with a maximum of 8.28 mm. Due to insufficient lateral reinforcing plates, the torsional deformation accumulates along the axis; The deformation gradient of the new top beam changes from small at the constrained end of the original top beam to a gentle transition, indicating that the optimization of lateral reinforcing plates effectively inhibits the propagation of torsional deformation. In the stress curve in Figure 17(b), the shear stress at the column socket of the original top beam increases with the increase of torsional deformation, and the curve shows an upward trend; Due to the longitudinal reinforcing plates being thickened to 40 mm (Design 2) in the new model, the rising amplitude of the curve decreases, the shear stress is dispersed along the height of the reinforcing plates, and the maximum peak stress decreases by 30.83 %.

On Path 2, the deformation near the column socket of the original top beam is slightly larger due to stress concentration, and the curve has a local bulge; The deformation of the new top beam is controlled in the column socket area due to the thickened longitudinal reinforcing plates improving the torsion-resistant support, and the deformation curve is more symmetrically distributed without obvious bulges. The stress curve of Path 2 shows that the stress asymmetry on both sides of the column socket of the original top beam is significant, and the curve is steep; Due to the design of reinforcing plates exceeding the cover plate (Design 4) in the new top beam design, the force flow is redistributed, the maximum stress peak decreases from 245.68 MPa to

## 227.11 MPa, and the smoothness of the curve is improved.

In summary, the design of the new top beam constructs a spatial torsion-resistant grid through dense layout of lateral reinforcing plates and heightening and thickening of longitudinal reinforcing plates, so that the torsion-resistant support of lateral reinforcing plates and the shear strengthening of longitudinal reinforcing plates form a collaborative effect, which not only inhibits the diffusion of torsional deformation, eliminates the risk of shear failure, but also reduces local stress through the optimization of force flow path, achieving a leap in mechanical properties under torsion conditions.

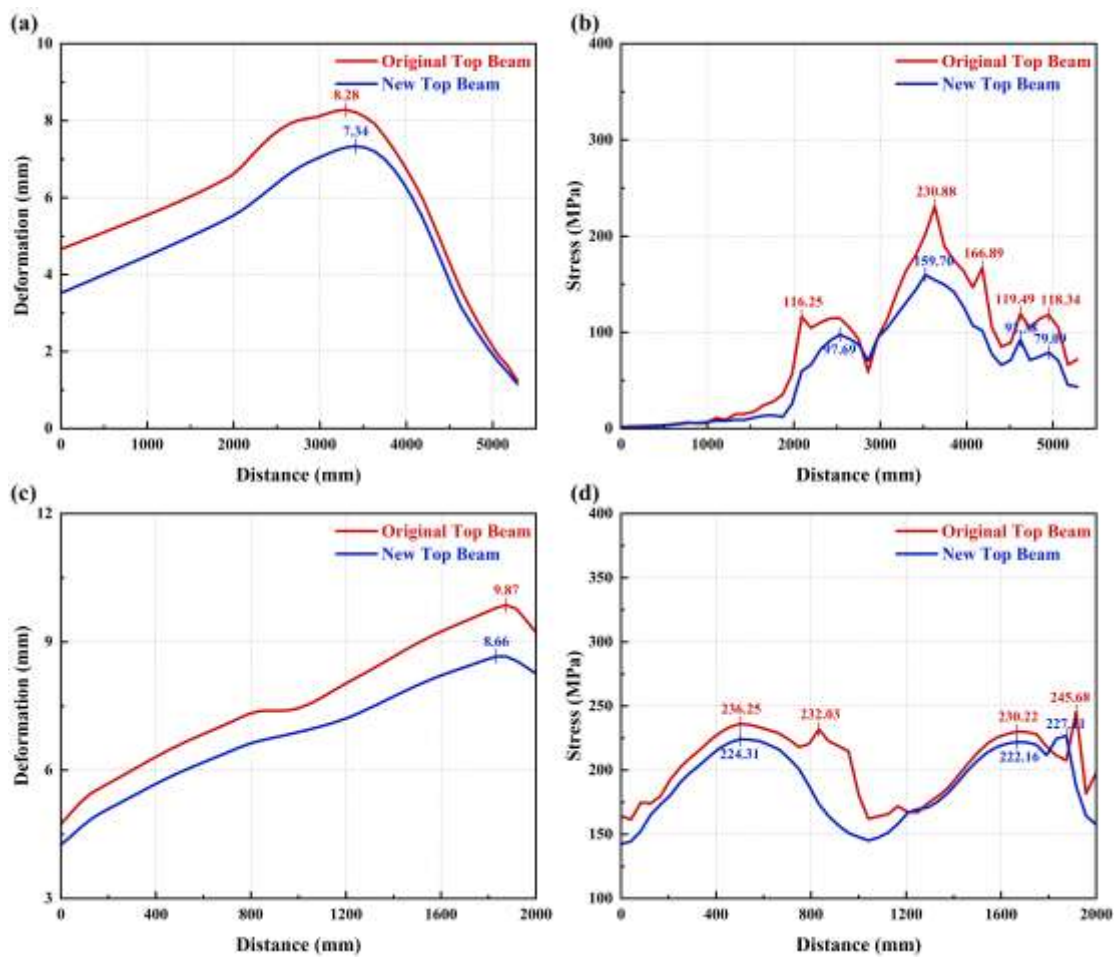


Figure 17 Total deformation and equivalent stress curves of old and new top beam top plates on two paths under diagonal torsion loading

(a) Total deformation nephogram of old and new top beams on Path 1; (b) Equivalent stress nephogram of old and new top beams on Path 1; (c) Total deformation nephogram of old and new top beams on Path 2; (d) Equivalent stress nephogram of old and new top beams on Path 2

## 3.2.3 Bending-Torsion Combination Working Condition

Under the bending-torsion combination condition, the original top beam has the worst mechanical properties due to bearing the superposition of bending and torsion loads. The maximum deformation reaches 25.48 mm, concentrated on the side without heel block support in the front, and the maximum equivalent stress is as high as 2436.9 MPa, far exceeding the yield strength of the material, with high stress areas distributed in the connection parts and edges; The optimized new top beam shows excellent resistance to composite loads under the combination condition. It can be seen from Figures 18(c)(d) that the maximum deformation is reduced to 21.498 mm, a decrease of 15.63 % compared with the original top beam, and the deformation in the front unsupported area is effectively controlled. In terms of stress, the maximum equivalent stress is reduced to 1774.2 MPa, which is 72.80 % of that of the original top beam.

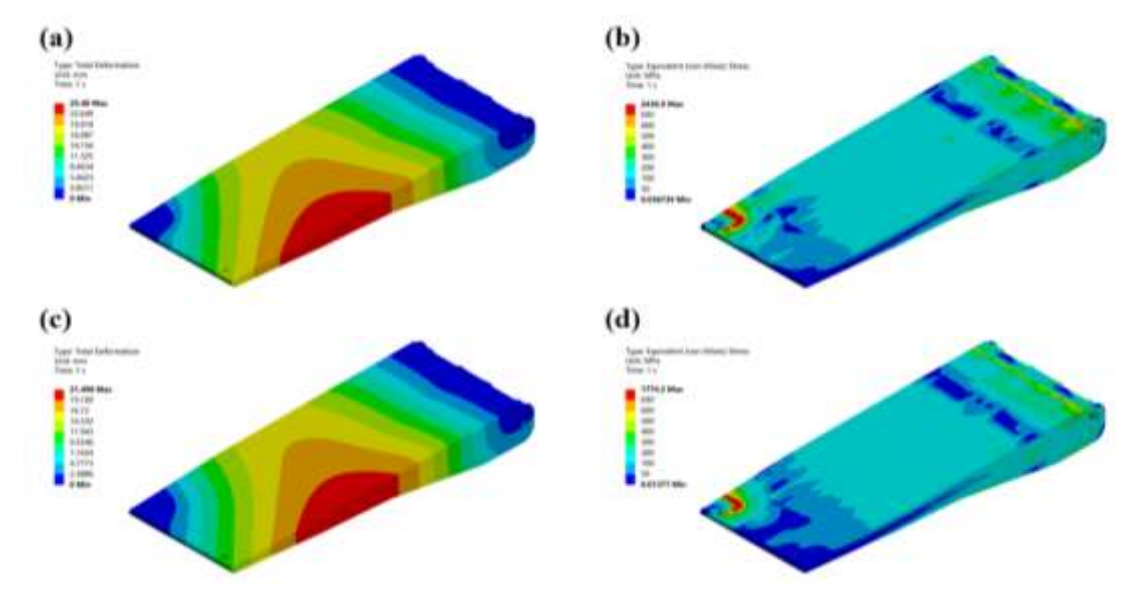


Figure 18 Total deformation and equivalent stress nephograms of old and new top beams under bending-torsion combination

(a) Total deformation nephogram of original top beam; (b) Stress nephogram of original top beam

ISSN: 0369-8963

(c) Total deformation nephogram of new top beam; (d) Stress nephogram of new top beam

The optimization effect can be clearly seen from the path curves in Figure 19. On Path 1, the original top beam has insufficient local stiffness due to the inner cover plate being only 12 mm and spliced by two pieces, which cannot resist composite deformation, with a maximum deformation of 21.03 mm. The new top beam has an improved stiffness and load-bearing area due to the inner cover plate being thickened to 25 mm and increased to four pieces (Design 4), the deformation is reduced to 17.83 mm, a decrease of 15.22 %, and the deformation curve is gentle. On the stress curve, the stress of the original top beam fluctuates greatly due to the superposition of midspan deformation caused by bending and diagonal deformation caused by torsion, with local stress increasing sharply. The new top beam, due to the collaboration of the integral steel plate and reinforcing plates, the distributed support of multiple cover plates disperses the local load caused by composite deformation, making the composite stress distribute uniformly, avoiding stress superposition, and the stress curve fluctuates less with reduced stress values.

As shown in Figures 19(c)(d), on Path 2, the deformation at the connection part between the column socket and the cover plate of the original top beam is slightly larger due to stress concentration, with a local bulge in the curve. The deformation curve of the new top beam has no obvious bulge because the connection between the inner cover plate and the reinforcing plates is strengthened, making the load transfer more stable. The maximum stress peak of the original top beam is 192.68 MPa, and the curve is steep, with weak connections due to the superposition of bending and torsion stresses. The new top beam, through adjusting the height of the reinforcing plates (Design 3),

ISSN: 0369-8963

makes the bending-torsion coupling stress transition smoothly, and the stress distribution range changes from local concentration of the original top beam to global dispersion.

From the optimization effects of the two paths, it can be seen that the optimization design scheme of the new top beam, aiming at the coupling effect of composite loads, focuses on the modular thickening of the inner cover plate and the gradient heightening of the reinforcing plates, expands the pressure-bearing surface, and constructs a collaborative mechanism of stiffness strengthening, force flow 疏导, and load dispersion: the inner cover plate strengthening resists local deformation, the integral steel plate ensures continuous force flow, and the topology optimization of the reinforcing plates guides stress distribution. The three work together to make the new top beam achieve the goals of controllable deformation and balanced stress under the bending-torsion combination condition.

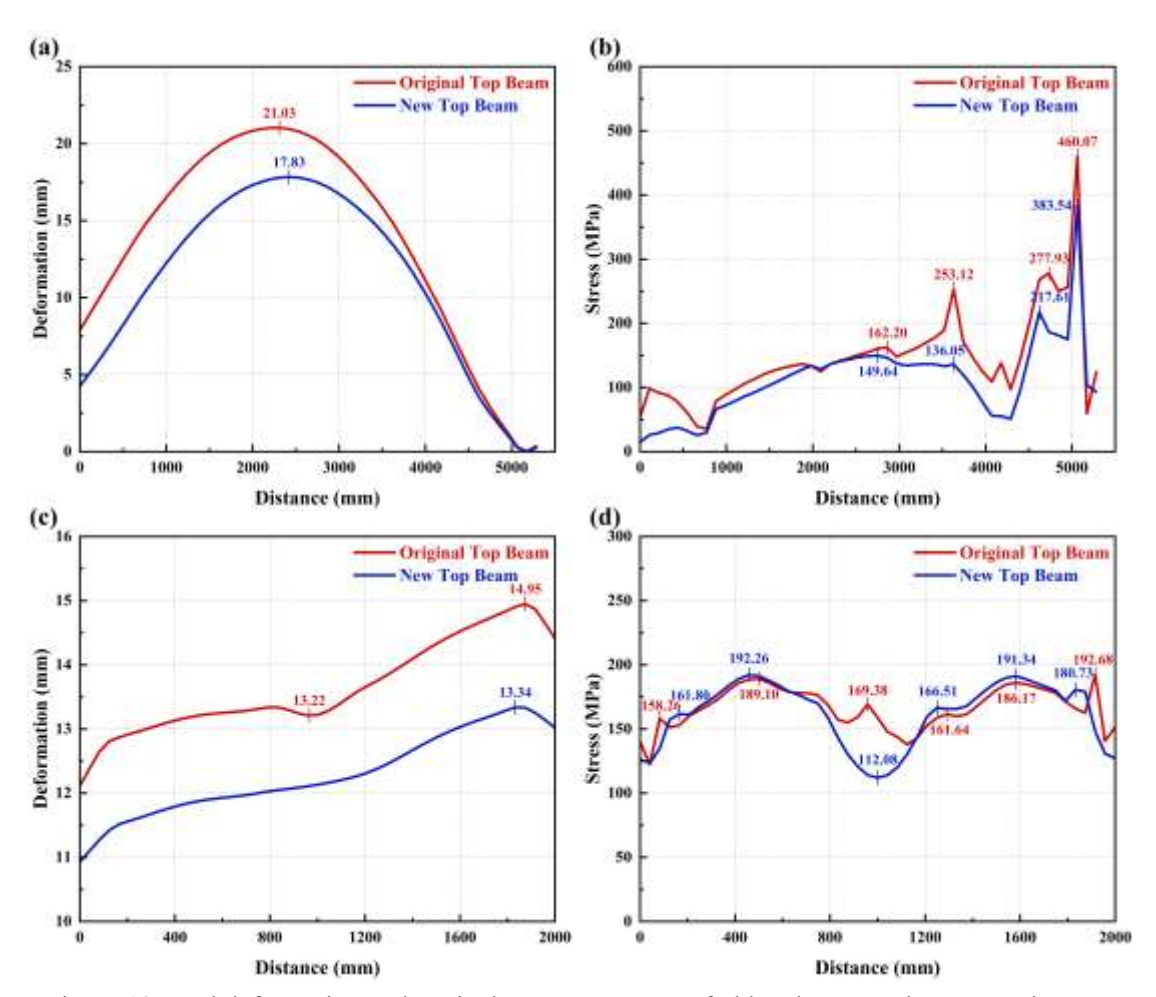


Figure 19 Total deformation and equivalent stress curves of old and new top beam top plates on two paths under bending-torsion combination loading

(a) Total deformation nephogram of old and new top beams on Path 1; (b) Equivalent stress nephogram of old and new top beams on Path 1; (c) Total deformation nephogram of old and new top beams on Path 2; (d) Equivalent stress nephogram of old and new top beams on Path 2

## 3.3 Comparative Verification of Test

Industrial practice is a key link to test the optimization effect of structural design. To verify the performance of the optimized new top beam structure in the actual working environment, an actual test study was conducted on the improved new top beam. The optimized new top beam structure was installed in the ZY14790/15/25D hydraulic support, and relevant loading tests were carried out for comparative verification, as shown in Figure 20.

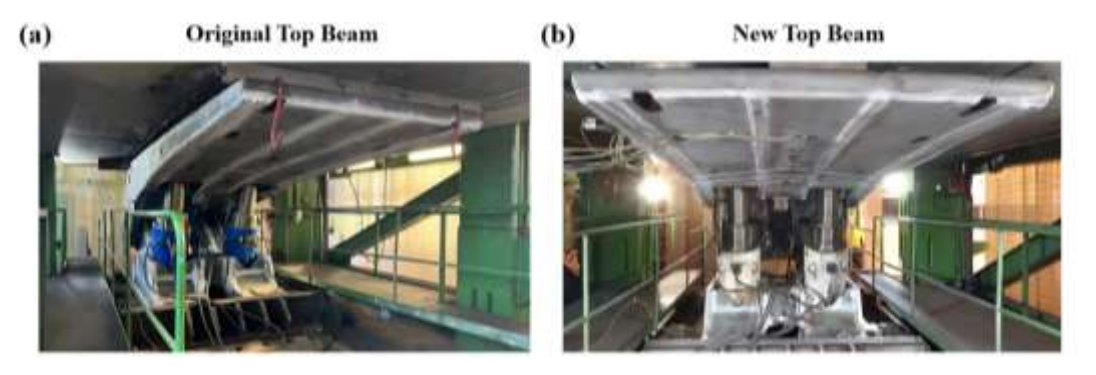


Figure 20 Cyclic loading test of old and new top beam models
(a) Engineering test of original top beam; (b) Engineering test of new top beam

## 3.3.1 Test of Original Top Beam

The test was based on 5000 cycle intervals, and the support was tested for 30000 cycles. Before the test, the support was inspected, non-destructively tested, and measured. At the end of each 5000 cycles, the top beam was measured and non-destructively tested. Before the test, the original top beam support had completed 2750 cycles in underground work. The test found that during the inspection at 7500 cycles, a crack was found on the lower surface of the main rib of the top beam, which was the first time a crack appeared on the surface of the top beam, with a length of less than 200 mm, and the crack did not mirror to the other side of the top beam. After completing 10000 cycles, the crack propagation at the crack position on the main support top beam was checked, as shown in Figure 21(c). The crack continued to propagate along the weld toe, and the total length of the weld crack was 430 mm at this time. In the 12000 cycle inspection, the previously identified crack position had propagated into the top beam base metal. As shown in Figure 21(b), two parallel lines entered the main vertical steel plate.

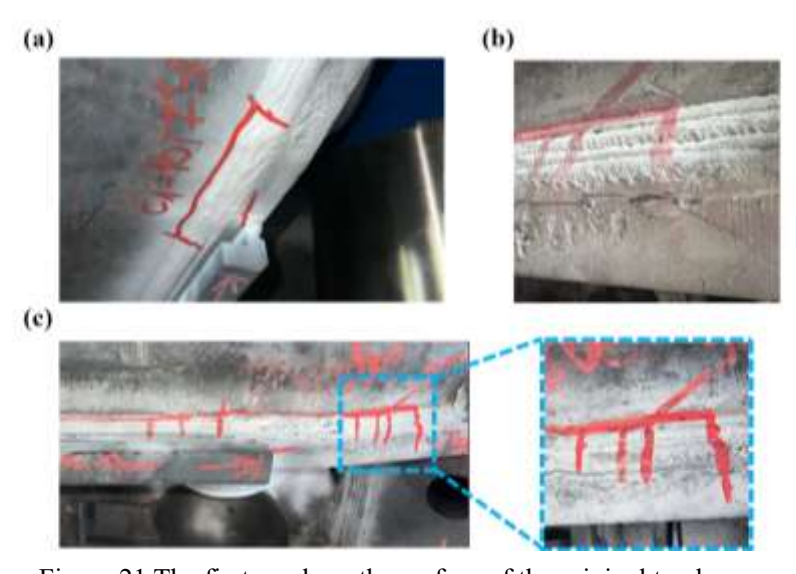


Figure 21 The first crack on the surface of the original top beam
(a) Crack on the surface of the original top beam; (b) Crack propagating to the base metal of the top beam; (c) Crack propagating along the weld toe

In the 15000 cycle inspection, non-destructive testing of the original top beam top plate found that the crack on the top beam top plate was consistent with the internal reinforcing plate, indicating that the crack at the joint between the reinforcing plate and the top plate had extended to the surface, as shown in Figure 22. The crack appeared on the top of the top beam, with a length of about 200 mm.

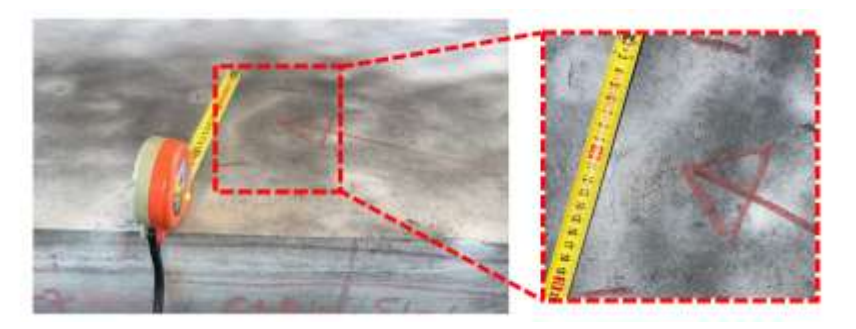


Figure 22 A crack with a length of about 200 mm on the original top beam top plate within 15000 cycles

In the 15000-20000 cycle test stage, the original top beam support fractured after 16,522 cycles and could not continue the test, with a total cycle count of 19272 for the original top beam. From the failure results, the top plate and the internal reinforcing plate fractured at the corresponding position, and there were welding defects inside,

ISSN: 0369-8963

leading to the original top beam structure being unable to bear the stress under longterm load, resulting in sudden fracture.



Figure 23 Fracture of the original top beam after 16522 cycles of test

## 3.3.2 Test of New Top Beam

Under the same conditions, a 30000-cycle test was conducted on the new top beam support. The test results showed that although the new top beam had weld cracks that propagated to the base metal at 19100 cycles, after standardized repair, it continued to complete the remaining 15000 cycles, and the total cycle count reached the test target. In addition, after 30000 cycles, the new top beam was measured and non-destructively tested, and the deformation met the acceptance criteria, and it could maintain the core function of safely supporting the full yield load, fully proving that the new top beam has better structural stiffness and deformation resistance. Compared with the original top beam, it can maintain stability under long-term load and has better fatigue performance.

The structural optimization and improvement work for the new top beam has achieved the expected effect. The optimized rear top beam is more stable in the actual working process, can create good economic benefits for enterprises, and plays an important role in promoting the performance improvement of coal mining equipment.

It not only provides a strong guarantee for the overall stability and safety of hydraulic supports but also provides a useful reference for the optimization and improvement of similar mechanical structures.

## 4. CONCLUSION

This paper takes the top beam of ZY14790/15/25D mine hydraulic support as the research core, aiming at the problem that the top beam is prone to failure due to complex loads in deep coal mining. A 3D simplified model is constructed using Solidworks, and static optimization and structural strengthening research are carried out under three typical working conditions: symmetric bending, diagonal torsion, and bending-torsion combination based on ANSYS software. The main work and conclusions are as follows:

- (1) In terms of mechanical characteristics analysis of the top beam under multiple working conditions, the original top beam has obvious stress concentration and deformation problems under the three working conditions: the maximum stress is 1966.8 MPa and the maximum deformation is 17.44 mm under symmetric bending conditions; the maximum stress is 1988.9 MPa and the maximum deformation is 13.517 mm under diagonal torsion conditions; the performance is the most prominent under bending-torsion combination conditions, with a maximum stress of 2436.9 MPa and a maximum deformation of 25.48 mm. High stress and large deformation areas are mainly concentrated in the connection parts and edges, becoming structural weak points.
- (2) In terms of top beam structure optimization and effects, aiming at the problems revealed by simulation, four structural optimization schemes are proposed: using a 40 mm integral steel plate to eliminate spliced welds, increasing the number of lateral

reinforcing plates and thickening longitudinal reinforcing plates to 40 mm, optimizing the layout of middle reinforcing plates, and thickening the inner cover plate to 25 mm and increasing to four pieces. After optimization, the mechanical properties of the top beam are significantly improved: the maximum stress decreases by 31.44% and the deformation decreases by 12.91% under symmetric bending conditions; the maximum stress decreases by 19.28% and the deformation decreases by 12.26% under diagonal torsion conditions; the maximum stress decreases by 27.20% and the deformation decreases by 15.63% under bending-torsion combination conditions, and the stress distribution is more uniform, achieving the goal of stress balance.

(3) In terms of test verification and industrial application value, the test shows that the original top beam fractures in advance during 30000 cycles of loading, while the optimized top beam can stably complete the test and the deformation meets the standard, verifying the reliability of the optimization scheme. This study provides technical support for the safe application of hydraulic support top beams in complex mine environments through multi-condition analysis and structural iterative design, and its optimization ideas also provide a reference for the design improvement of similar load-bearing structures.

## 5. REFERENCES

- [1] Wang J. Development and prospect on fully mechanized mining in Chinese coal mines[J].

  International Journal of Coal Science & Technology, 2014, 1: 253-260.
- [2] Xinhua Liu, Guofa Wang, Chengfeng Liu. The entire frame of two columns large mining height hydraulic support finite element analysis. Coal Science and Technology, 2010,38 (8): 93-94.

- ISSN: 0369-8963
  - [3] DUAN Mengjie. Corrosion failure analysis and preventive measures of hydraulic support column[J]. Hebei Coal, 2002(5): 28-29.
  - [4] LI Chenyang, LAN Zhiyu, CHENG Xiangbang, et al. Failure analysis and preventive measures of hydraulic support column jack[J]. Coal Mining Machinery, 2020, 41(2):146-148.
  - [5] ZHANG Xiaowei,MA Juntao,HUANG Xin,et al. Cause analysis and improvement measures of cracks in mining pillar socket[J]. Coal Mining Machinery,2015,36(7):235-236.
  - [6] WANG Benghai. Damage analysis of ZY7600/24/50 shield hydraulic support[J]. Coal Mining Machinery,2010,31(8):208-209.
  - [7] LI Junlong,LIU Hunju,PAN Xuerong. Fracture failure analysis of hydraulic support pin[J]. Coal Mining Machinery,2013,34(6):99-101.
  - [8] XIA Zhongqiu. Finite element analysis on mechanical properties of key components of hydraulic support[D]. Fuxin: Liaoning University of Engineering and Technology,2007.
  - [9] Hongyu L ,Xun F .Computer simulation and model test research on strength test of hydraulic support[J].THIRD INTERNATIONAL SYMPOSIUM ON PRECISION MECHANICAL MEASUREMENTS,2006,628062803W-62803W-6.
  - [10] CHEN Jing. Research on strength reliability optimization design method of hydraulic support[D].
    Xuzhou:University of Mining and Technology,2014.
  - [11] General Administration of Quality Supervision, Inspection and Quarantine of the People's Republic of China, Standardization Adiministration of the People's Republic of China. GB/T 25974.2—2010, Powered support for coal mine-Part 2: Specification for power set legs and rams[S]. Beijing: China Standard Press, 2011.
  - [12] He W ,Chen Z ,Du J , et al. Finite Element Analysis of Combination Condition of ZF6400/19/32

- Hydraulic Support[J].IOP Conference Series: Materials Science and Engineering, 2019, 490(5):
- [13] Zhao X ,Li F ,Liu Y , et al.Fatigue Behavior of a Box-Type Welded Structure of Hydraulic Support Used in Coal Mine[J].Materials,2015,8(10):6609-6622.
- [14] Bing Xu, XiangZe Liu .ZFS6000-20-36 Hydraulic supports top beam design and force analysis Coal Mine Machinery, 2010,31 (5): 32-33.
- [15] PeiSi Zhong, Jiandong Song, Mei Liu. ANSYS-based thin seam roof cover hydraulic support. Coal Mine Machinery, 2011,32 (4): 84-85.
- [16] He W, Chen Z, Du J, et al. Finite Element Analysis of Combination Condition of ZF6400/19/32 Hydraulic Support[C]//IOP Conference Series: Materials Science and Engineering. IOP Publishing, 2019, 490(5): 052006.
- [17] Wang Wei, Optimization Design of Top Beam of ZY3400/17/39 Hydraulic Support Based on Topology Optimization[J].Mechanical Management and Development. 2020, 35(10): 65-66.
- [18] Hu D G, Fan X. Analysis of the strength and reliability of hydraulic support with finite element method[J]. Advanced Materials Research, 2013, 619: 225-230.
- [19] ZHANG Wei. Analysis of common failure forms and Countermeasures of hydraulic support used in coal mine[J]. Coal Mining Technology, 2017,22(6):22-25.